Planck-LFI 4K reference Load:

Reference Horn Design and Optimization

F. Cuttaia, A. Brighenti, P. Calzolari, G. Cazzola,
N. Mandolesi, S. Mariotti*, G. Morigi, M. Sandri,
L. Valenziano, F. Villa

Internal Report n° 392
Te.S.R.E., July 2004

*IRA-CNR

1 Introduction

This short note describes the process of reference horn optimization. Data are obtained at 44 and 30 GHz, since we can build and test prototypes at these frequencies. Dimensions are then scaled at 100 GHz. The 70 GHz reference horn has been modeled in the same way, but it is not scaled.

The main goals of the horn design optimization are:
Return Loss <≈ -25 dB
Small main beam pattern in the near field
Sidelobe level below –40 dB in the near field in the area of the reference target

2 Simulation Method

A new simulation method (called *hybrid* method), based on the mode-matching approximation, is developed to model the field distribution at the aperture of small pyramidal horns.

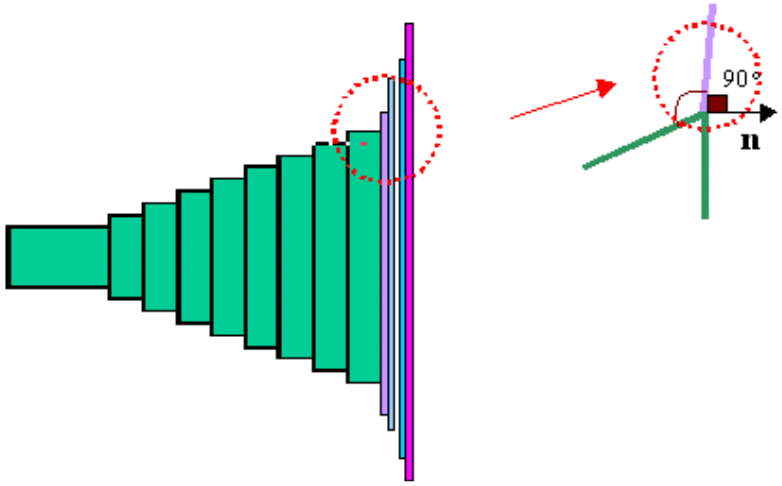

Figure 2.1: Sketch of the hybrid method approximation

The horn aperture is modeled in two subsequent regions, as illustrated in Figure 2.1: the first one is the horn flare (green region); the second one is the plate around the aperture. This is modeled as a series of infinitesimal thin steps, which approximate the plate. In other terms, the discontinuity at the aperture is represented by a flare with an angle of approximately 90°. This approximation is then validated on experimental data and compare with other methods.

This method is validated on data in the literature and then compared to test results of 4KRL horns at 30 and 44 GHz. One of the main difficulties is to simulate the plate, present in the units under test, around the horn aperture. The effect of this feature is not represented by the simple mode-matching method.

Once the field distribution at the aperture is known, the antenna pattern is evaluated using the GTD approximation. GRASP-8 package is used, under some assumptions, for this purpose.

2.1 Method validation

Hybrid method is first compared with the standard mode-matching (MM) approximation on a experimental Return Loss data of a pyramidal horn whose dimensions are large compared with the wavelength.

a	b	A	B	Lf	θ_H	θ_E	Δs
WR22 WG dimensions		Aperture H-plane	Aperture E-plane	Flare length	Flare angle H-plane	Flare angle E-plane	thickness
mm					deg		mm
5.69	2.845	34.4	25.9	37.750	20.820	16.981	0.9

Table 2.1: Standard horn dimensions: Flare length is the distance from the WG to the aperture. The thickness is referred to the horn wall thickness

As is easily seen from Figure 2.2 the hybrid method is able to reproduce the shape of the data, provided that the plot is shifted by 1.5 GHz. This effect is expected for such simulations [1].

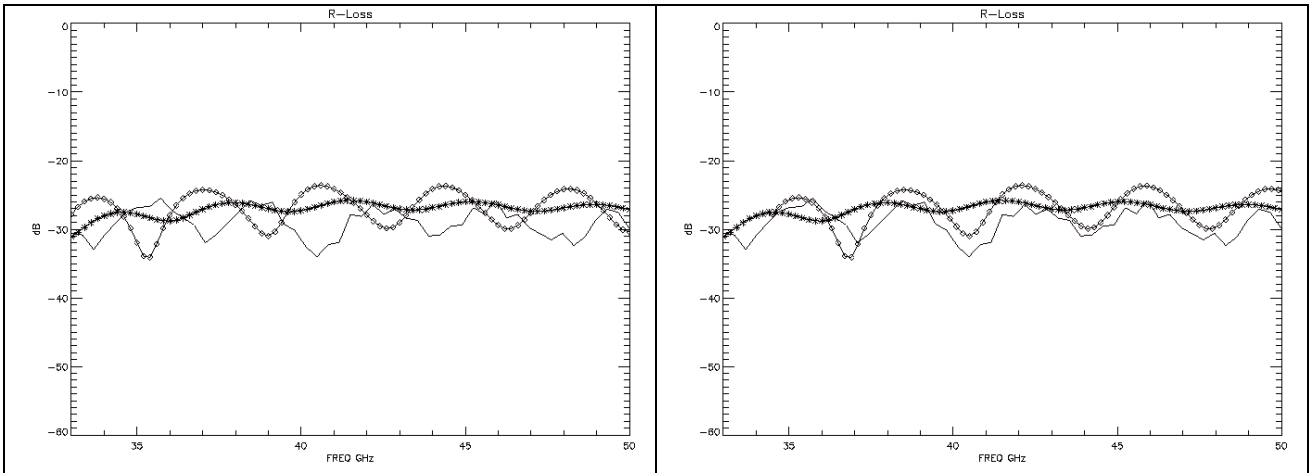

MM (***), hybrid method (□), measured data (-----)

MM (***), hybrid method (□), measured data (-----). The hybrid method plot is shifted by 1,5

Figure 2.2 Simulation method (Hybrid method, mode-matching) comparison with experimental data on a standard pyramidal horn. Simulated data on the right panel are shifted by 1.5 GHz. MM indicates the mode-matching.

However, the mode-matching simulation is less accurate in the case of small antennas [1].
The hybrid method was therefore validated and on data taken from the literature [1], referred to small pyramidal horn [1]. Horn dimensions are reported

a	b	A	B	Lf	θ_H	θ_E	Δs
WR75 WG dimensions		Aperture H-plane	Aperture E-plane	Flare length	Flare angle H-plane	Flare angle E-plane	thickness
inch					deg		inch
0.75	0.375	1.355	1.355	3.06	5.64	9.1	0.05

Table 2.2: Data used for the model validation on small pyramidal horns (from [1])

Experimental data are best modeled by the Method of Moments (MoM), while the mode-matching fails (Figure 2.3, right panel). It can be seen from the left panel of Figure 2.3 that the hybrid method is more accurate in representing the general features of the measured data.

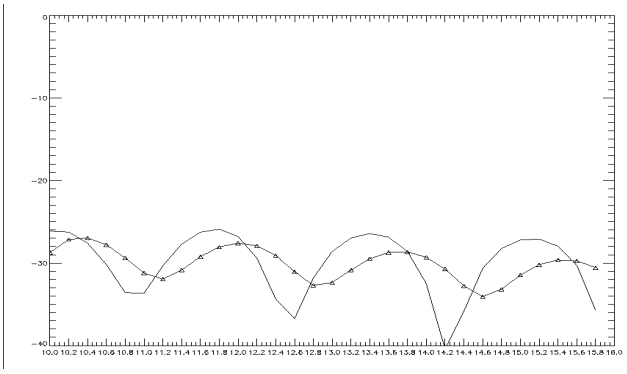

Simulation comparison (hybrid method (continous line) and mode matching (***)

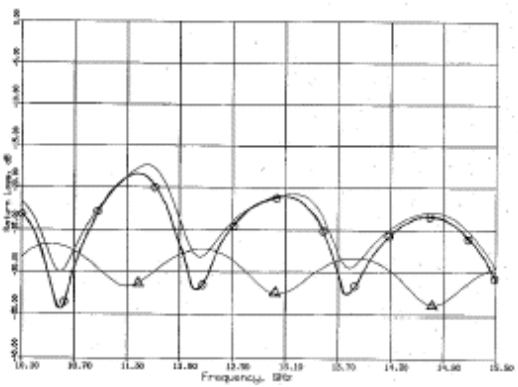

Bhattacharyya: Mode Matching vs MoM

Figure 2.3: simulation method comparison with literature data.
Data are in 10 GHz band (10.1-10.5 GHz)

This method is compare with standard mode-matching (MM) and experimental data.

In conclusion, the hybrid method is able to recover measured data of small pyramidal horns much better than the standard mode-matching approximation. It is therefore applicable for the 4KRL antennas.

2.2 Return Loss of the 4KRL antennas

We then simulated the Return Loss of the 4KRL antennas (model EBB) at 30 and 44 GHz and compared them with measured data. Test results show a sufficient, even if qualitative, agreement with the simulations, as shown in Figure 2.4, Figure 2.5. The effect of considering the plane around the aperture is evident. The mode-matching method is not able to reproduce the data, while the hybrid method can be applied, as a first approximation, to discriminate between different horn design.

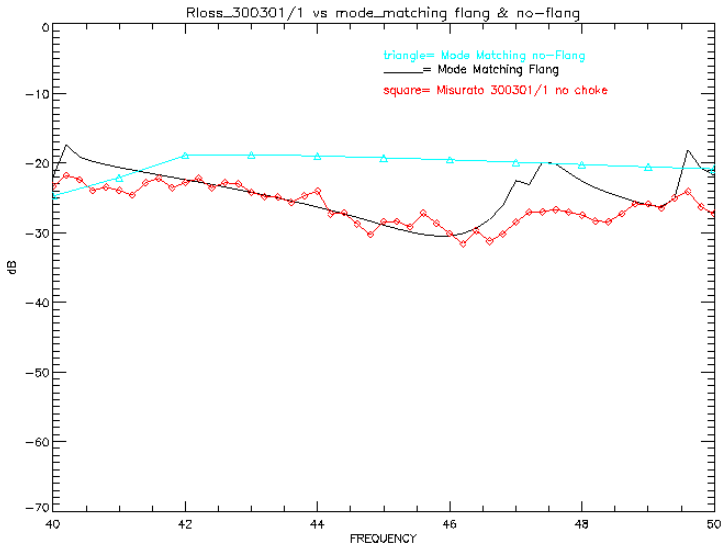

Figure 2.4: Prototype simulation and test at 44 GHz for the design 'EBB'. Light blue curve is the simulation without the plane around the aperture.. Continuous black line is the simulation including the plane. Red curve reports measured data.

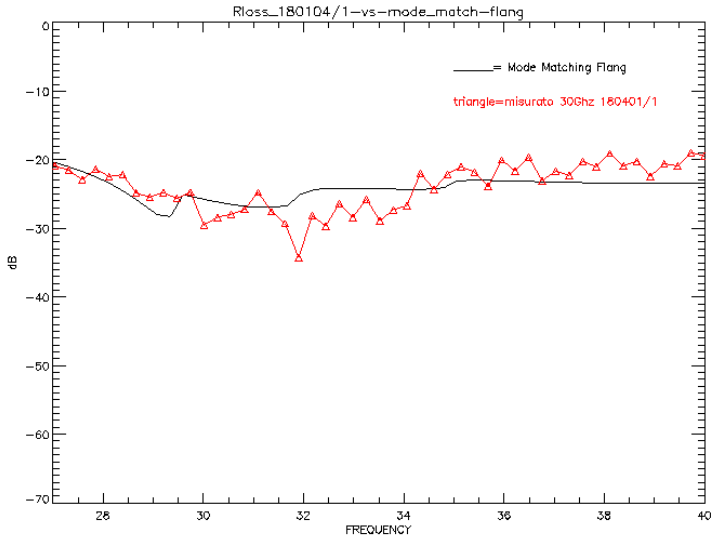

Figure 2.5: Same as above for the 30 GHz reference horn model 'EBB'. Only the simulation including the plane is reported.

2.3 Pattern simulations

Horn near-field pattern in not easy to be modeled. We therefore developed a combined method: fields at the aperture of the horn are obtained by the hybrid method. This fields are then propagated using the GRASP-8 package. The accuracy of the hybrid method was discussed above, while the GRASP-8 software is a standard for pattern simulations in the far field. We first validated the combined method by reproducing the far field pattern of standard antennas [from 2]. Antenna parameters are reported in Table 2.3 and Table 2.4.

a	b	A	B	Lf	λ
22.86	10.16	40.13	29.21	51.05	29.3

Table 2.3: parameters of the antenna@10GHz 10dB standard-gain horn

a	b	A	B	Lf	λ
22.86	10.16	67.564	49.53	138.68	29.3

Table 2.4: parameters of the antenna @10GHz, 15dB standard-gain horn

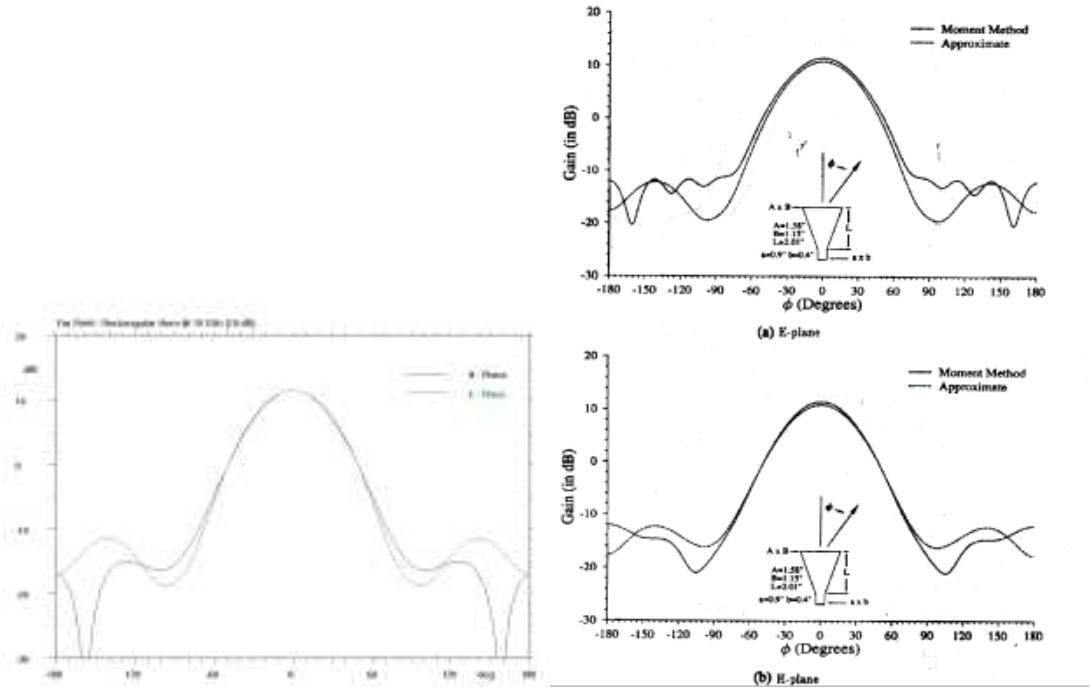

Figure 2.6: Right panel: Antenna pattern (10 dB standard horn at 10 GHz) from [2]. Left panel: results of the hybrid method simulations and GRASP-8 modeling. The agreement is satisfactory.

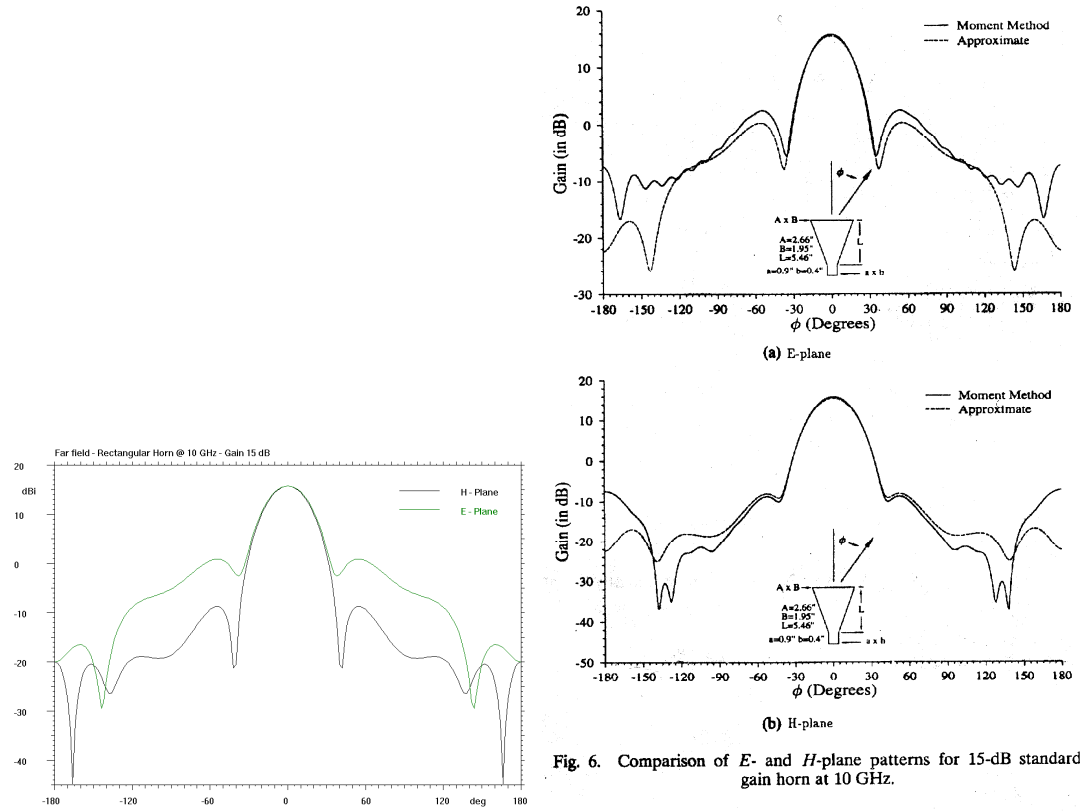

Figure 2.7: Right panel: Antenna pattern (15 dB standard horn at 10 GHz) from [2]. Left panel: results of the hybrid method simulations and GRASP-8 modeling. The agreement is satisfactory.

It can be seen even from a visual comparison of Figure 2.6 and Figure 2.7, that the agreement is satisfactory. Therefore the field at the aperture, calculated using out hybrid method, can be used as input to the GRASP-8 package for propagation.

2.4 Comparison with measured data of a small pyramidal horn

We than moved to test the combined method, in the far-field, for one of the 4KRL pyramidal horn. This test is needed to verify the reliability of the simulation method on small pyramidal antennas. The Far-field pattern of small pyramidal horns (model NEW040 and LAB, see following section for design details) has been measured in the anechoic chamber and compared with our simulations and with a method described in [3].

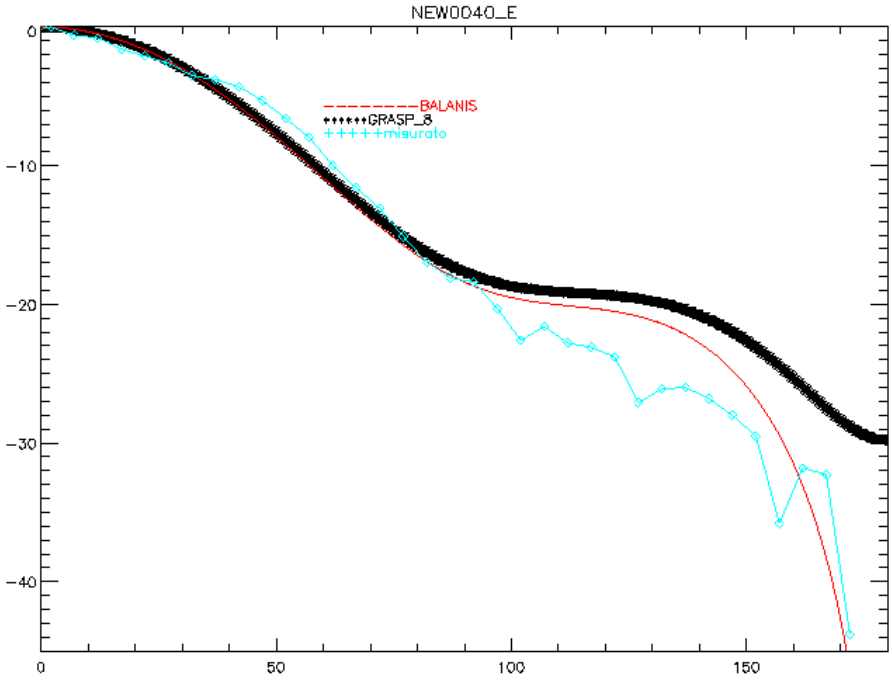

Figure 2.8: Comparison between measured data (light blue) of the NEW040 horn in the E-plane with two simulation methods: Hybrid method+GRASP8 (black line) and [3] (red line).

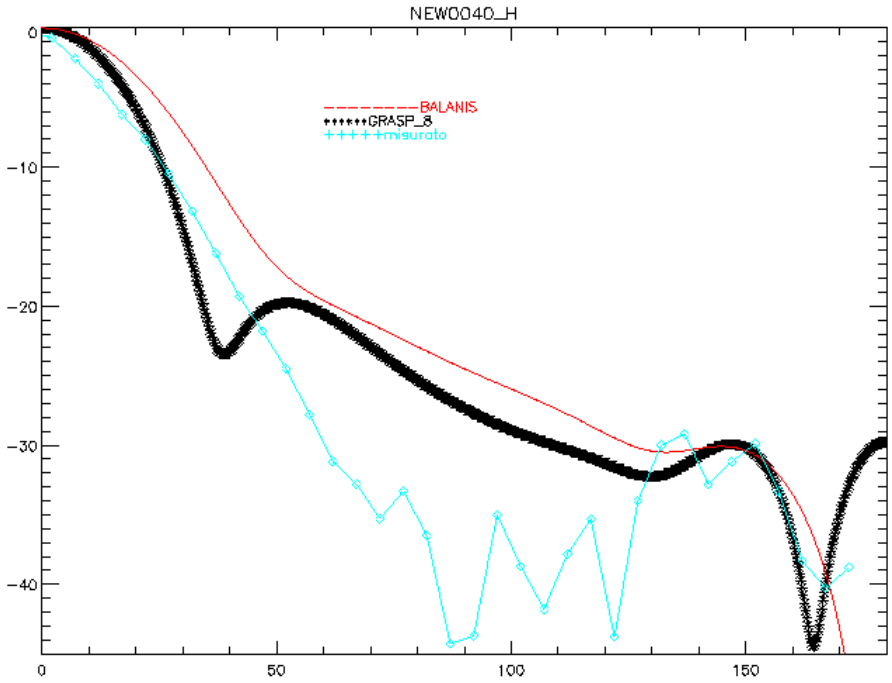

Figure 2.9: Comparison between measured data (light blue) of the NEW040 horn in the H-plane with two simulation methods: Hybrid method+GRASP8 (black line) and [3] (red line).

The simulation includes another method (form [3]) to calculate the fields at the aperture for the sake of comparison.
The agreement is quite good in the main lobe region of the E-plane (up to about 90 deg), while both simulations methods overestimate the pattern at larger angles (Figure 2.8).
Simulations of the H-plane are not in agreement with measured data.

This behavior can be attributed to two main problems:

- Both methods are not accurate in reproducing pyramidal antennas with dimensions small with respect to the wavelength.
- The horn used for this measurements have a plane around the aperture. This latter feature can be modeled with our method.

We built a new small test horn (called LAB), whose flare length is longer than in the NEW040 one. We machined one of the test horn to reduce the plate around the aperture (this model is called LAB-A). The difference between the model is reported in Figure 2.10.

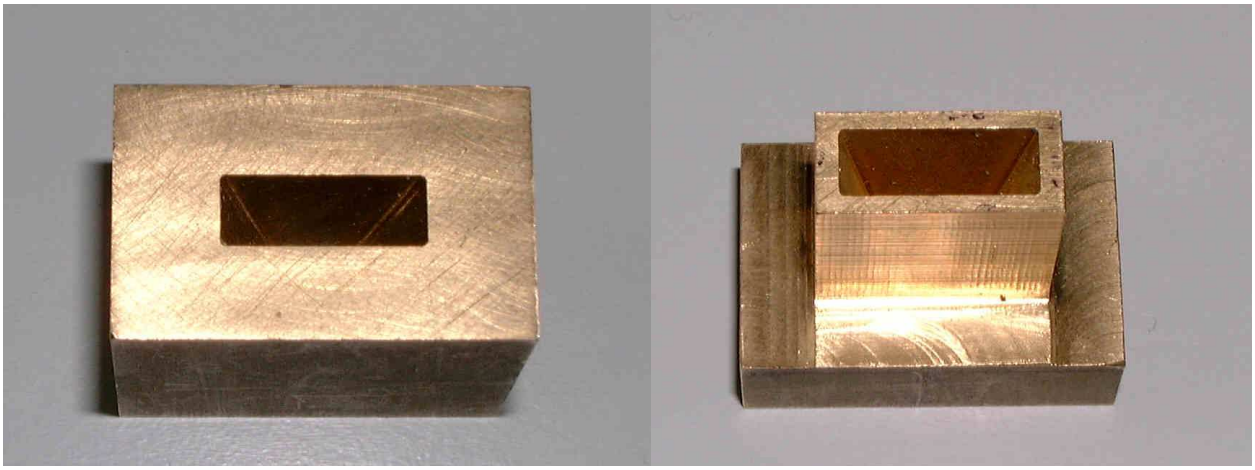

Figure 2.10: Left panel: horn model LAB, band 44 GHz. Right panel: horn model LAB-A, band 44 GHz. Note that the plate around the aperture has been machined out on the LAB-A model

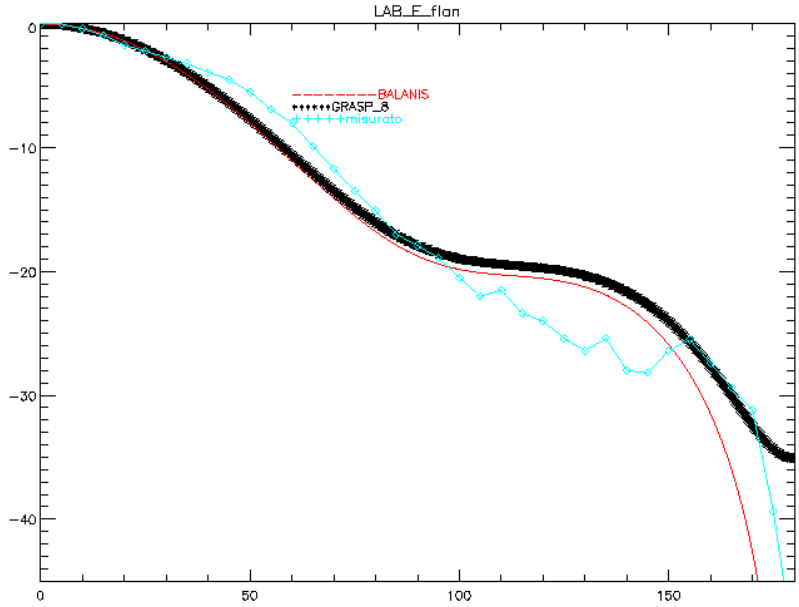

Figure 2.11: Comparison between measured data (light blue) of the LAB horn, **with** the plane around the aperture, in the E-plane with two simulation methods: Hybrid method+GRASP8 (black line) and [3] (red line).

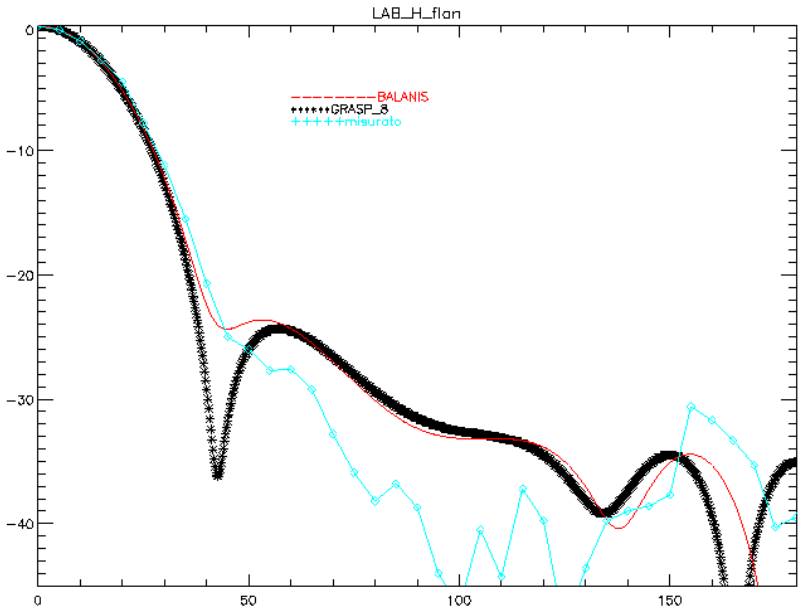

Figure 2.12: Comparison between measured data (light blue) of the LAB horn, **with** the plane around the aperture, in the H-plane with two simulation methods: Hybrid method+GRASP8 (black line) and [3] (red line).

In the case of a LAB horn with the plane the agreement between the simulation and the data is much better (Figure 2.11 and Figure 2.12) then in the previous case (Figure 2.8 and Figure 2.9).
We now evaluate the effect of the plane around the aperture, by comparing the results from the horn LAB (Figure 2.11 and Figure 2.12) and LAB-A (Figure 2.13 and Figure 2.14).

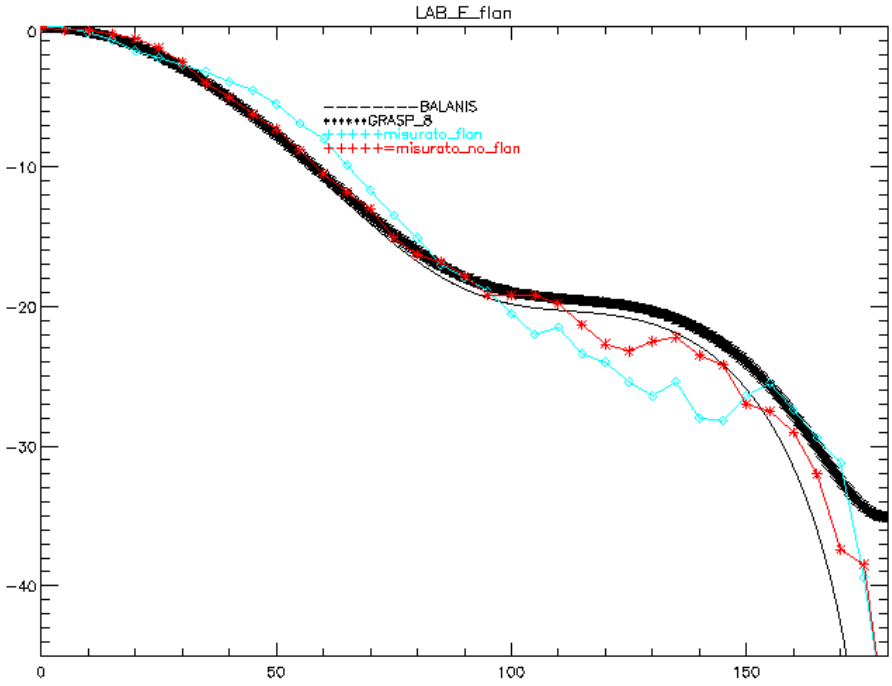

Figure 2.13: Comparison between the simulation and measured data (E-plane) of the horn *model LAB* with the plane around the aperture (light blue) and without the plane LAB-A (red). Hybrid method+GRASP8 (thick black) and method from [3] (thin black) are over-plotted.

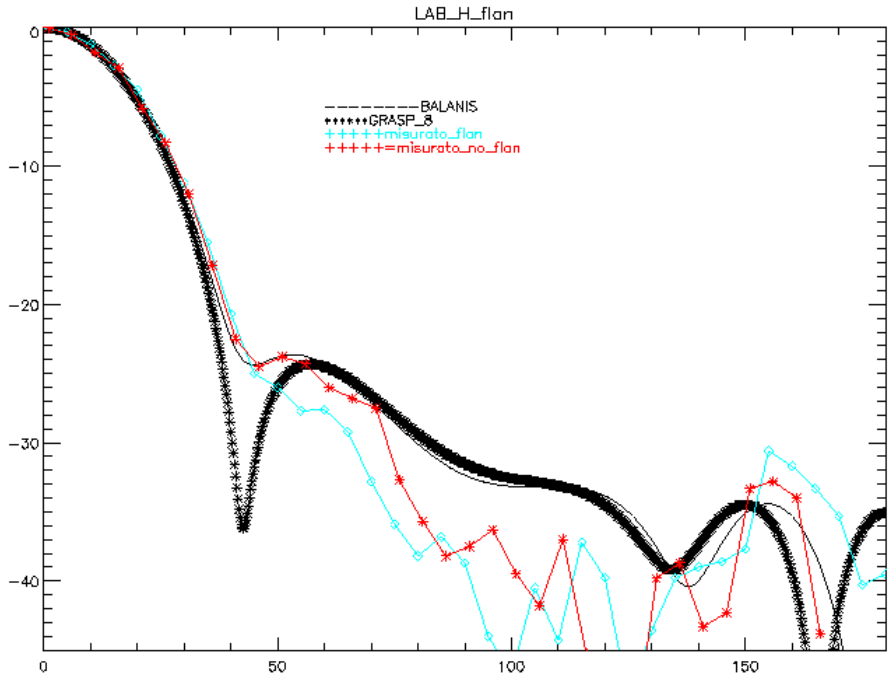

Figure 2.14: Comparison between the simulation and measured data (H-plane) of the horn *model LAB* with the plane around the aperture (light blue) and without the plane LAB-A (red). Hybrid method+GRASP8 (thick black) and method from [3] (thin black) are over-plotted.

The effect of the plane is particularly evident in the H-plane (Figure 2.14), where the simulations systematically overestimate the pattern.

We can therefore conclude that our simulations cannot represent the experimental data with high accuracy. Nonetheless, they can be considered a worst case approximation of the measured data. We consider that sufficient for the purpose of evaluating new horn design.

The further assumption is that the GRASP-8 package is accurate in modeling the near-field pattern of pyramidal horns, which is extremely difficult to measure.

3 Optimization of Reference Horn for the 4KRL

3.1 Design

We then simulated the return loss of the pyramidal antenna for the 4KRL as a function of the aperture dimensions, flare angles in the two planes and flare length. The limits for these parameters were set according to the maximum envelope allowed by mechanical design of FEMs. More than 2000 configurations were modeled and only those fulfilling the requirement on RL < -30dB (without plane around the aperture) were selected. Between them, two candidates have been identified: the first one (EBB-long) has the same aperture dimensions of the 'EBB' one, but a longer flare; the second one (NEW-0040) has a smaller aperture and a longer flare with respect to the 'EBB' horn. A third horn (LAB) has been selected to test the simulation method and the effect of the plane around the aperture (see previous section). We then included the effect of the plane around the aperture in the model. These final model (one for each candidate horn) is to be compared with test results.

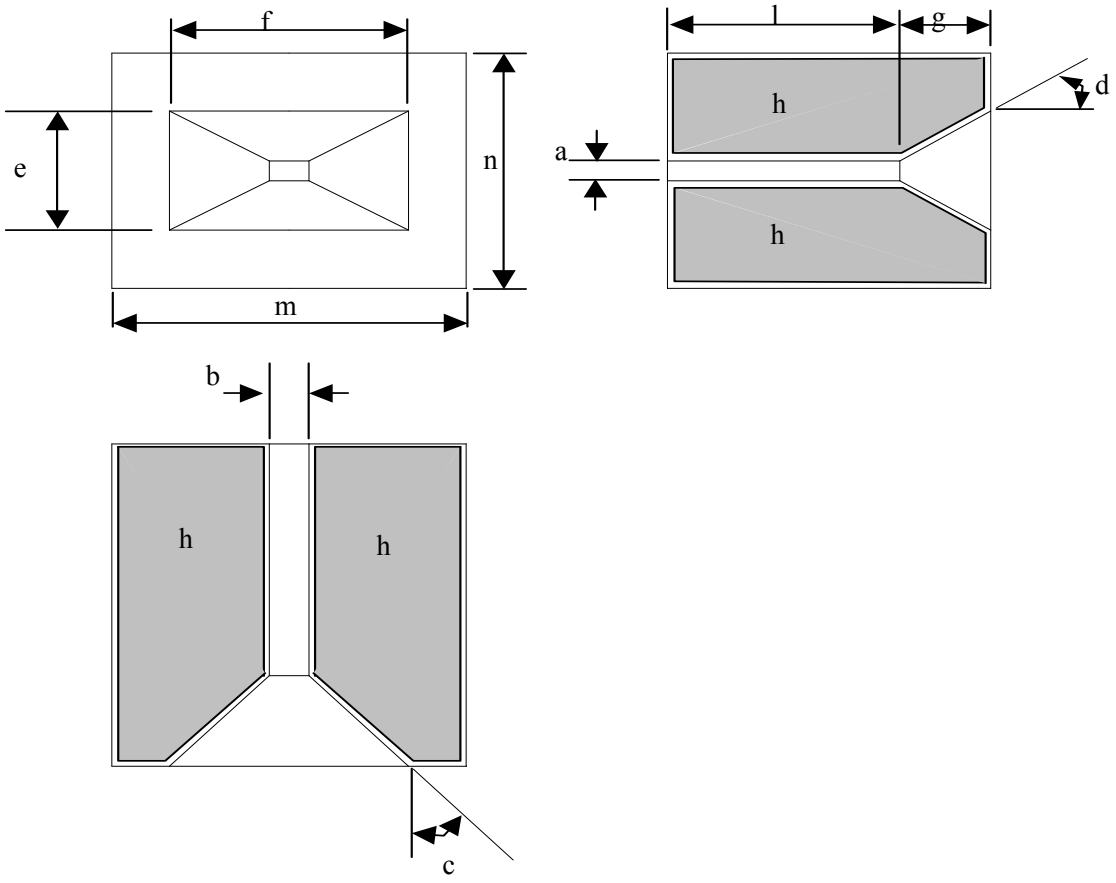

Figure 3.1: Sketch of the horn dimensions. This figure includes the dimensions of the plane around the horn aperture. Labels refer to Table 3.1.

In Table 3.1 the dimensions of the horn are reported.

Design	Freq	a	b	c	d	e	F	g	m	n
Units	(GHz)	mm		deg		mm			Plane (mm)	
NEW0040	100	1.270	2.540	33.915°	10.537°	2.360	6.480	2.930	19.05	19.05
EBB	70	1.550	3.100	47.570	28.682	4.629	9.257	2.814	19.05	19.05
EBB	44	2.845	5.69	47.569	28.680	7.365	14.730	4.13	30	19.04
EBB-long	44	2.845	5.690	34.084	18.691	7.365	14.730	6.68	30	19.04
NEW0040	44	2.845	5.690	34.084	10.681	5.365	14.730	6.68	30	19.04
LAB	44	2.845	5.690	12.710	3.597	5.365	14.730	20.04	30	19.04
LAB-A	44	2.845	5.690	12.710	3.597	5.365	14.730	20.04	20.730	11.365
EBB	30GHz	3.560	7.120	47.566	28.680	10.800	21.600	6.62	30	19.04

Table 3.1: Dimensions of the horn built for the 4KRL optimization. Column labels refer to Figure 3.1.

3.2 Return Loss of the new reference horns

The measured Return Loss of the NEW040 horn is presented in Figure 3.2. Data show a sufficient agreement with the simulations. Ripples in the measured traces can also be attributed to the non-ideal calibration of the network, as it is shown in Figure 3.2, where a laboratory matched load is measured. A flat trace would have expected if the calibration was ideal.

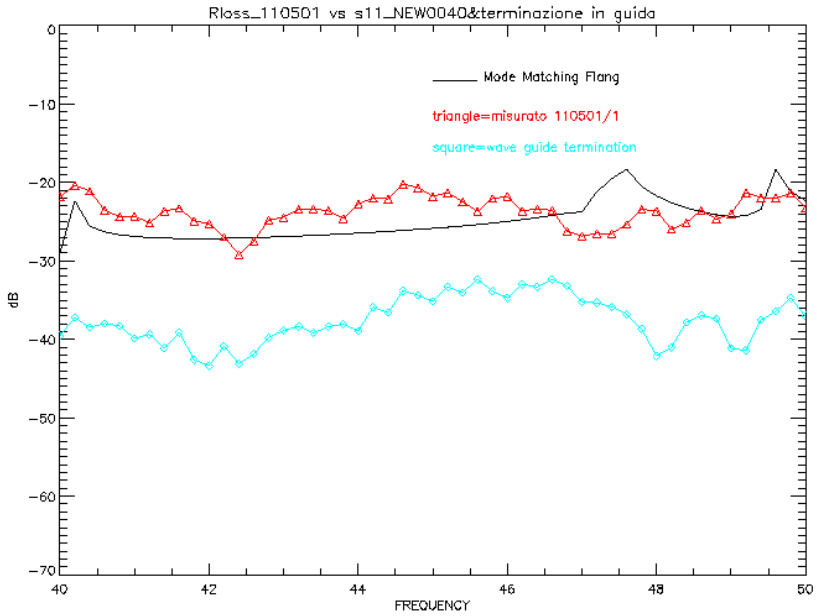

Figure 3.2: Return Loss of the NEW-040 horn in the 44 GHz band. Red curve are measured data, continuous black is the simulation including the plane around the aperture. Light blue curve is the RL of a matched load, showing *non-ideal* calibration of the network chain.

The Return Loss of the EBB-long model is presented in Figure 3.3.

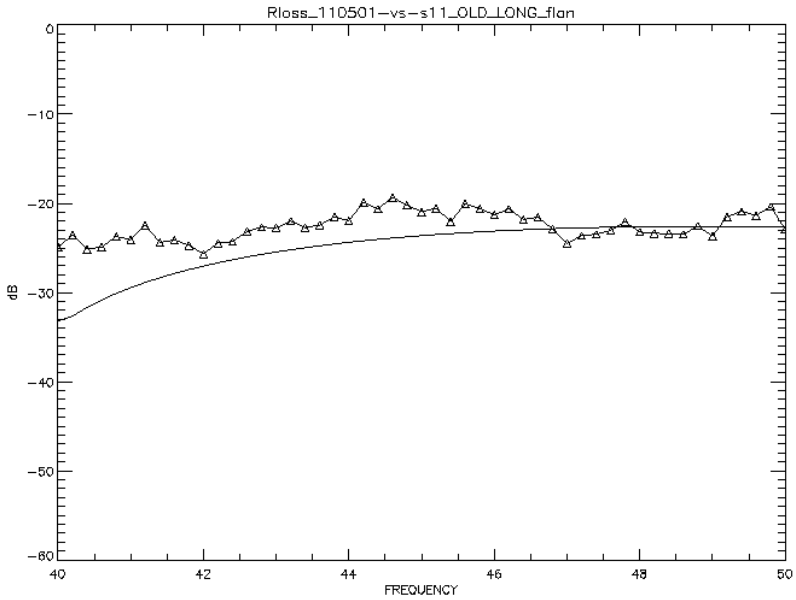

Figure 3.3: Return Loss of the EBB-LONG model. Triangles are measured data, continuous black line are simulated data.

By comparing the results presented in Figure 2.4, Figure 3.2 and Figure 3.3 some considerations can be drawn:

- Return Loss average value of the three candidate reference horn are comparable.
- The model NEW-040 shows a flatter RL in the band, while a resonance is present in the two other models (EBB and EBB-LONG).

3.3 Pattern

We have shown in previous sections that the accuracy of our simulations is sufficient for the purpose of the horn optimization. Simulation results are compared with measured data, once a new horn design is selected. We make here the assumption that the GRASP-8 package is accurate in modeling the near-field pattern of the small pyramidal horns. We then calculate the near-field pattern of the EBB-long design and of the NEW040 design.

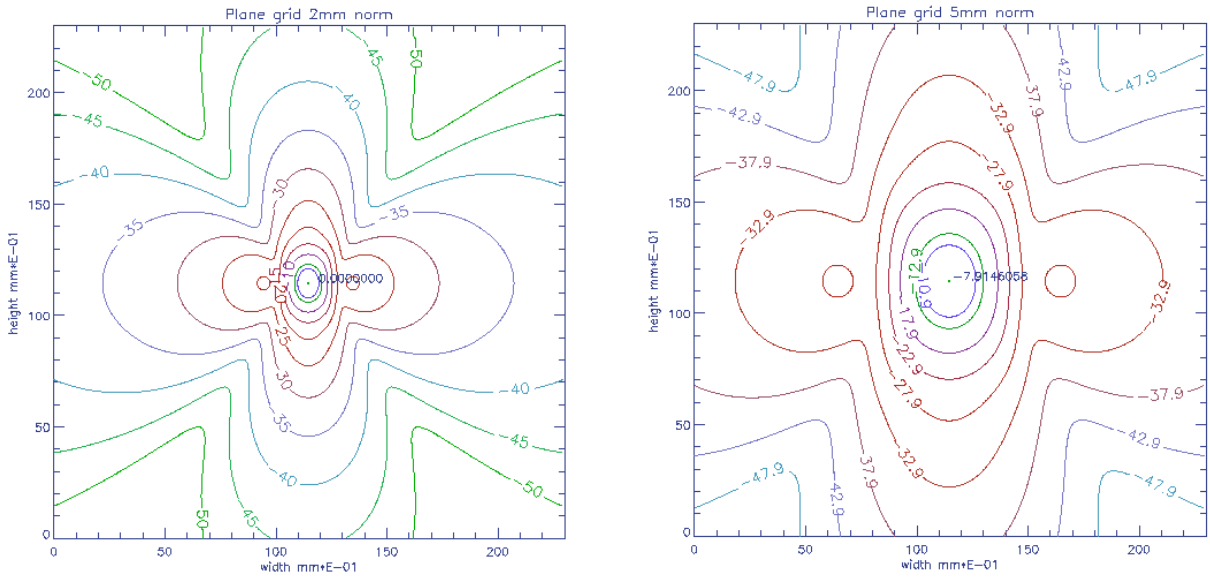

Figure 3.4: Contour plots of the pattern of the EBB-long horn design at 44 GHz. Left panel is at d=2mm from the aperture. Right panel is at 5 mm. Data are normalized at d=2mm. Axis (box-side) length show the actual dimension of the reference target.

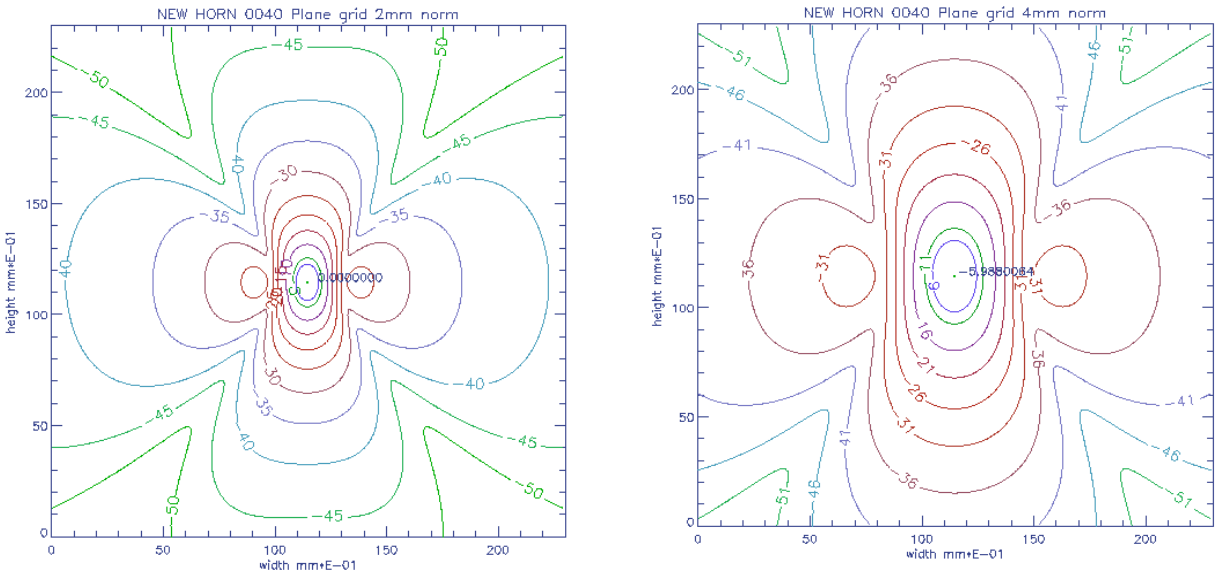

Figure 3.5: Same as above for the NEW040 design. Note that at d=2 mm (left panel) the –40 dB contour is completely inside the target area.

The NEW-040 field pattern at 2 mm distance from the aperture shows the –40dB contour inside the reference target projected dimensions, while the EBB and EBB-LONG ones have the same contour partially outside it.

4 Discussion

The design of small pyramidal horn is not an easy task and can not follow the standard rules for antenna design [1]. Dedicated simulations must be implemented, as it was done for the reference horns of the 4KRL. In particular the gold-rule of the 1:2 ratio of the aperture dimensions in the H-E planes of the horn is not automatically applicable in the case of such small horns. Considerations on the near-field pattern (which proved to be more confined with smaller horn aperture) must be taken into account.

From the results presented in the previous sections, especially those on near-field pattern (assuming the Return Loss not significantly improved), we consider the NEW-040 horn design the best one between the tested models for the following reasons:

- The RL characteristics is flatter than the for the other models especially when measured with the reference target.
- The field pattern is more confined and this will improve the leakage of the horn-target system

The NEW-040 horn is therefore selected to be included in the QM of the LFI.

Bibliography

1. A.K.Bhattacharyya, G.Z.Rollins *Accurate Radiation and Impedence Characteristics of Horn Antennas- A Moment Method Model*, IEEE Trans. on Antennas Propagation, **44**, No 4, 1996
2. K.Liu, C.Balanis, G. Barber**,** *Analysis of pyramidal Horn Antennas Using Moment Methods*, IEEE Trans. on Antennas Propagation, Vol **41**, No 10, 1993
3. C.Balanis, *ANTENNA THEORY, Analysis and design*, Wiley